Silence of IGFBP7 suppresses apoptosis and epithelial mesenchymal transformation of high glucose induced-podocytes

XIAOJUN CAI, LEI WANG, XULING WANG and FENGYAN HOU

Department of Endocrinology, Heilongjiang Provincial Academy of Chinese Medical Science, Harbin, Heilongjiang 150036, P.R. China

Received November 8, 2017; Accepted February 16, 2018

DOI: 10.3892/etm.2018.6298

Abstract. Insulin-like growth factor-binding protein 7 (IGFBP7) has been identified as a secreted protein associated with a number of cellular processes. However, the specific regulatory mechanisms of IGFBP7 on podocytes of diabetic nephropathy (DN) are yet to be elucidated. In the present study, podocytes were identified initially via an immunofluorescence assay using an anti-synaptopodin antibody. It was subsequently demonstrated that glucose promoted podocyte proliferation in a time- and dose-dependent manner via MTT assay. In addition, IGFBP7 expression was silenced in podocytes via siRNA, the effects of which were evaluated using western blotting and reverse transcription-quantitative polymerase chain reaction. It was demonstrated that silencing IGFBP7 inhibited apoptosis and epithelial mesenchymal transformation (EMT) of podocytes mediated by high glucose (HG). Transforming growth factor (TGF)-β1/mothers against decapentaplegic homolog (Smad) signaling was associated with proliferation, apoptotic activities and EMT. Therefore, the expression levels of TGF-β1/Smad pathway were detected, and it was observed that silencing IGFBP7 suppressed the TGF-β1/Smad pathway in podocytes induced by HG. These findings suggested that IGFBP7 may serve as a potential therapeutic target for DN.

Introduction

Diabetic nephropathy (DN) is a microvascular complication of diabetes that is clinically characterized by proteinuria (1). Previous studies have demonstrated that podocytes have a vital role in the induction of proteinuria, which contributes to DN (2-4). Podocytes are located in the glomerular basement membrane outside the glomerular capillaries (5). Proteinuria was separated from proteinuria podocytes and apoptosisoccursin glomerularbasement membrane (6,7). However, previous studies have demonstrated that podocyte detachment and apoptosis occur prior to proteinuria (6,8). It has also previously been indicated that podocyte dysfunction may serve as a pathway contributing to proteinuria via epithelial-to-mesenchymal transition (EMT) (9,10). Blocking EMT has also been indicated to reverse podocyte apoptosis in its early phase (9,11). Thus, these findings may provide a novel pathway to alleviate DN.

Podocytes are terminally differentiated visceral epithelial cells that are located outside the glomerular capillaries where they form the final filtration barrier to protein loss (12-14). In diabetic nephropathy, podocytes injury leads to the disruption of the filtration barrier and protein leakage. The loss of podocytes has been indicated as an important early pathologic marker (15-17). Accumulating evidence suggests that EMT is a possible engagement for podocyte depletion in diabetic nephropathy. During EMT, epithelial cells are transformed to mesenchymal cells in response to injurious stimuli (11,13,16).

Insulin-like growth factor binding protein 7 (IGFBP7) is a member of the IGF binding protein family, and is able to regulate cell proliferation, differentiation, angiogenesis, cell adhesion and cellular senescence in a variety of cells (18-23). Furthermore, silence of IGFBP7 is associated with poor post-operative survival in various types of cancer, such as glioma, liver and colorectal cancer (24-27). However, the effects of IGFBP7 on apoptosis and EMT of high glucose induced-podocyteshave are yet to be elucidated.

In the present study, podocytes were identified and the role of IGFBP7 on cell proliferation, apoptosis and EMT of podocytes mediated by high glucose was analyzed. The expression levels of transforming growth factor (TGF)-β1/mothers against decapentaplegic homolog (Smad) pathway were also detected, and it was observed that silencing IGFBP7 inhibited the TGF-β1/Smad pathway in podocytes induced by high glucose. These findings suggest that IGFBP7 may serve as a potential therapeutic target for DN.

Materials and methods

Cell culture. Human podocytes (cat. no. BNCC340460) were obtained from the Type Culture Collection of the Chinese

Correspondence to: Dr Xiaojun Cai, Department of Endocrinology, Heilongjiang Provincial Academy of Chinese Medical Science, 41 Xiangshun Street, Xiangfang, Harbin, Heilongjiang 150036, P.R. China
E-mail: xiaojuncai25jc@163.com

Key words: insulin-like growth factor binding protein 7, transforming growth factor-β1/mothers against decapentaplegic homologpathway, podocytes, high glucose

Academy of Sciences (Shanghai, China). Podocytes were cultured in an incubator (95% humidity, 5% CO_2) at 37˚C for 48 h in Ham's F12 nutrient mixture-Dulbecco's modified Eagle's medium (Thermo Fisher Scientific, Inc., Waltham, MA, USA) with 10% fetal bovine serum (Gibco; Thermo Fisher Scientific, Inc.) and 1% penicillin-streptomycin G (Invitrogen; Thermo Fisher Scientific, Inc.).

Cell treatment. Podocytes ($3x10^5$ cells/ml) were seeded in 6-wells plates, and treated with PBS and glucose at 5, 10, 20, 40, 60, 80 or 100 mM at room temperature. The podocytes were then transferred to the incubator and held for 6, 12, 24 and 48 h at 37˚C. Negative control small interfering (si)RNA (siNC; 5'-ACGUGACACGUUCGGAGAATT-3') and siRNA against IGFBP7 (siIGFBP7; 5'-CATCCAATT CCCAAGGACAG-3') vectors were chemically synthesized by Shanghai GenePharma Co., Ltd. (Shanghai, China) and prepared for transfection. Podocytes were plated in 6-wells plates at a density of $1x10^6$ cells per well. The vectors (50 nM) were transfected into podocytes using Lipofectamine® 2000 (Invitrogen; Thermo Fisher Scientific, Inc.) for 48 h according to the manufacturer's instructions. following 48 h transfection, experiments were performed.

RNA extraction and reverse transcription-quantitative polymerase chain reaction (RT-qPCR). Total RNA was isolated using TRIzol (Invitrogen; Thermo Fisher Scientific, Inc.) following the manufacturer's protocol and reverse transcribed to cDNA assay using an miScript II RT kit (Qiagen GmbH, Hilden, Germany). The mRNA expression levels were measured using the SYBR-Green PCR Master Mix kit (Takara Biotechnology Co., Ltd., Dalian, China). The target genes and GAPDH were analyzed by RT-qPCR using an ABI 7500 system (Applied Biosystems; Thermo Fisher Scientific, Inc.). The thermocycling conditions were as follows: Pre-degeneration, 90˚C for 10 min; (denaturation, 90˚C for 40 sec; annealing, 62˚C for 35 sec, for 30 cycles) extension, 72˚C for 30 sec. Primers were designed as follows: IGFBP7 forward, 5'-GTGGCCCAGAAA AGCATGAA-3' and reverse, 5'-AAGTTGGGTATAGCTCGG CA-3'; apoptosis inducing factor (AIF) forward, 5'-CCCAAT GTTGAGTTGGCCAA-3' and reverse, 5'-AGCGTGATCATG GTGCTCTA-3'; caspase-3 forward, 5'-TTGCCACCTGTC CAGTTTTG-3' and reverse, 5'-AGGAGTGAGTGGTCTTGC TC-3'; caspase-9 forward, 5'-GCCCCATATGATCGAGGA CA-3' and reverse, 5'-CAGAAACGAAGCCAGCATGT-3'; nephrin forward, 5'-ACCGTGAGCTCCTTCTATCG-3' and reverse, 5'-CATTCCACAGATGCAGAGCC-3'; phosphorylated (p)-cadherin forward, 5'-GAGAAGGAGACAGGCTGG TT-3' and reverse, 5'-GGGTAAACTTGGGCTTGTGG-3'; fibroblast-specific protein (FSP)-1 forward, 5'-GAGAAGGAG ACAGGCTGGTT-3' and reverse, 5'-GGGTAAACTTGGGCT TGTGG-3'; α-smooth muscle actin (SMA) forward, 5'-CTG GGGAGTTGGAAGCAGTA-3' and reverse, 5'-CTGTTT CACAAGCCCCTCAC-3'; Snail forward, 5'-AGTGGTTCT TCTGCGCTACT-3' and reverse,5'-GTAGGGCTGCTGGAA GGTAA-3'; TGF-β1 forward, 5'-GTGGTGATCATGGAA GACGC-3' and reverse, 5'-TTGTGGTCAGGATTCTCG CT-3'; and Smad7 forward, 5'-TAGCCGACTCTGCGAACT AG-3' and reverse, 5'-CACTCTCGTCTTCTCCTCCC-3'; GAPDH forward, 5'-GTGGAGTCTACTGGCGTCTT-3' and reverse, 5'-CCTTCCACGATGCCAAAGTT-3'. Data were quantified applying the $2^{-\Delta\Delta Cq}$ method (28). The relative mRNA expression levels were normalized to GAPDH. 3 independent experiments were performed, and the mean data collected was calculated.

Western blot analysis. An RIPA buffer (Beyotime Institute of Biotechnology, Haimen, China) was used to lyse cells, according to the manufacturer's protocol, and a BCA Protein Assay kit (Thermo Fisher Scientific, Inc.) was applied to detect the protein concentrations. Equivalent proteins (25 μg) were separated by 10% SDS-PAGE and transferred to a polyvinyl difluoride (PVDF) membrane (PerkinElmer, Inc., Waltham, MA, USA). PVDF membranes were subsequently blocked for 2 h at room temperature with 5% non-fat dry milk and incubated with the following primary antibodies overnight at 4˚C: Anti-GAPDH (1:2,000; cat. no. ab8245), anti-IGFBP7 (1:1,000; cat. no. ab74169), anti-AIF (1:1,000; cat. no. ab1998), anti-cleaved (c)-Caspase-3 (1:1,500; cat. no. ab13586), anti-c-Caspase-9 (1:1,500; cat. no. ab25758), anti-nephrin (1:1,000; cat. no. ab58968), anti-p-cadherin (1:1,000; cat. no. ab19350), anti-FSP-1 (1:2,000; cat. no. ab40722), anti-α-SMA (1:1,000; cat. no. ab5694), anti-Snail (1:1,000; cat. no. ab53519), anti-TGF-β1 (1:1,000; cat. no. ab92486), anti-Smad7 (1:1,000; cat. no. ab55493), anti-p-Smad3 (1:1,000; cat. no. ab52903) and anti-smad3 (1:1,000; cat. no. ab40854; all Abcam, Cambridge, UK). Subsequently, the PVDF membranes were incubated with secondary antibody [horseradish peroxidase conjugated (HRP) mouse anti-rabbit immunoglobulin G (IgG); 1:5,000; cat. no. sc-2357; Goat anti-mouse IgG-HRP; 1:6,000; cat. no. sc-2005; Donkey anti-goat IgG-HRP; 1:6,000; cat. no. sc-2020; each Santa Cruz Biotechnology, Inc., Dallas, TX, USA] for 1 h at room temperature. The results were analyzed using the enhanced chemiluminescence substrate kit (GE Healthcare, Chicago, IL, USA) and the automatic chemiluminescence image analysis system (Tanon 4200; YPH-Bio, Beijing, China).

Cell proliferation assay. An MTT assay was performed to determine the proliferation of podocytes exposed to various treatments. The treated cells ($3x10^3$ cells/well) were seeded in a 96-well plate and cultured for 6, 12, 24 and 48 h at 37˚C. Next, cells were incubated with 20 μl MTT (5 mg/ml) solution for 4 h at 37˚C and 10 μl dimethyl sulfoxide (cat. no. 6-68-5; MOLBASE Biotechnology Co., Ltd., Shanghai, China) was added to dissolve the formazan. The absorbance was measured at 490 nm using a microplate reader.

Cell apoptosis analysis. Podocytes ($5x10^4$ cells/well) were seeded in 6-well plates and cultured at 37˚C for 24 h. Then, cells were treated with PBS (Control), siNC, high glucose (HG; 60 mM), siNC and HG, or siIGFBP7 and HG for 12 h. Cells were subsequently centrifuged (1,000xg, 5 min, 4˚C) and fixed for 2 min in 70% (v/v) ethanol on ice. According to the manufacturer's protocol, the cells were double-stained using an Annexin V-fluorescein isothiocyanate/propidium iodide kit (BD Biosciences, Franklin Lakes, NJ, USA) for 20 min at room temperature in the dark. Samples were immediately analyzed for apoptosis using a FACSCalibur flow cytometer (BD Biosciences). The data was analyzed by the ModFit

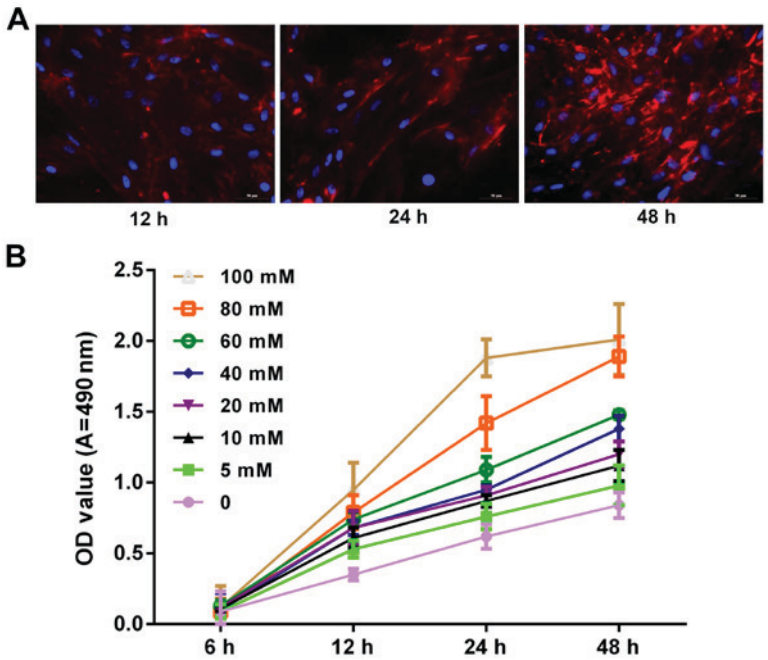

Figure 1. Glucose promoted podocyte proliferation in a marked time- and dose-dependent manner. (A) Podocytes were cultured at 37˚C for 12, 24 and 48 h. The synaptopodin expression was detected using immunofluorescence assay. The cells were visualized under fluorescence microscopy. Blue and red fluorescence represents the nucleus and synaptopodin, respectively. (B) MTT assay was performed to measure the proliferation of podocytes treated with PBS and glucose at 0, 5, 10, 20, 40, 60, 80 and100 mM for 6, 12, 24 and 48 h. OD, optical density; A, absorbance.

LT 2.0 software (Verity Software House, Inc., Tophsham, ME, USA).

Immunofluorescence staining. Podocytes ($5x10^4$ cells/well) were seeded in 6-well plates and cultured at 37˚C for 12, 24 and 48 h. Then, cells were washed with PBS and fixed with 4% paraformaldehyde at 4˚C for 20 min. The fixed cells were washed with PBS for 3 times, and permeabilized with 0.2% Triton X-100 for 3 min. Cells were subsequently washed with PBS, and blocked with 10% goat serum (Shanghai Haoran Biological Technology Co., Ltd., Shanghai, China) for 30 min at 37˚C. The anti-synaptopodin antibody (1:600; cat. no. ab220345; Abcam) was used to incubate with the cells overnight at 4˚C. Following washing with PBS in triplicate, cells were incubated with an Alexa-Fluor 633-conjugated secondary antibody (1:5,000; cat. no. A20005; ThermoFisher Scientific, Inc.) at room temperature for 1 h. DAPI (Thermo Fisher Scientific, Inc.) was then added to stain the nuclei at room temperature for 15 min. Finally, samples were evaluated under fluorescence microscopy (magnification, x200; Olympus Corporation, Tokyo, Japan).

ELISA. TGF-β1 concentration was analyzed using an ELISA kit (cat. no. SX01158; Shanghai Senxiong Biotech Industry Co., Ltd., Shanghai, China), according to the manufacturer's protocol. Podocytes ($5x10^4$ cells/well) were seeded in 6-well plates and cultured in at 37˚C for 24 h. cells were then treated with PBS (Control), siNC, high glucose (HG; 60 mM), siNC and HG, or siIGFBP7 and HG for 12 h at 37˚C. Diluted standard product (20 μl) was prepared. Enzyme reagent (100 μl) was added for 30 min at 37˚C, and subsequently color agent (100 μl) was added to plates for 15 min at 37˚C. Finally, the reaction was terminated using termination liquid (50 μl). Subsequently, the absorbance (OD value) was measured at 450 nm using a microplate reader. A standard curve was produced using GraphPad prism 7 software (GraphPad Software, Inc., La Jolla, CA, USA) and the different concentrations of samples were obtained by comparing the OD value of the samples to the standard curve.

Statistical analysis. Data were analyzed using SPSS 19.0 software (IBM Corp., Armonk, NY, USA). Significant differences between groups were assessed using one-way analysis, and the post hoc LSD test was performed. Data are presented as the mean ± standard deviation. $P<0.05$ was considered to indicate a statistically significant difference.

Results

Glucose promotes podocyte proliferation in a time-dependent and dose-dependent manner. To explore whether glucose is associated with the progression and development of podocytes, the expression level of synaptopodin in podocytes was measured via immunofluorescence assay. Blue and red staining represented the nucleus and synaptopodin, respectively. Results demonstrated that synaptopodin staining at 48 h was deeper than that of 12 and 24 h. This indicated that synaptopodin was highly expressed in podocytes (Fig. 1A). In addition, podocytes were treated with PBS and glucose at 0, 5, 10, 20, 40, 60, 80 and 100 mM for 6, 12, 24 and 48 h. The results indicated that the proliferation ability of podocytes increased with increasing dosage and time (Fig. 1B).

IGFBP7 silencing in podocytes via siRNA. To further determine the exact roles of IGFBP7 in podocytes, IGFBP7 expression was blocked via transfection with siIGFBP7.

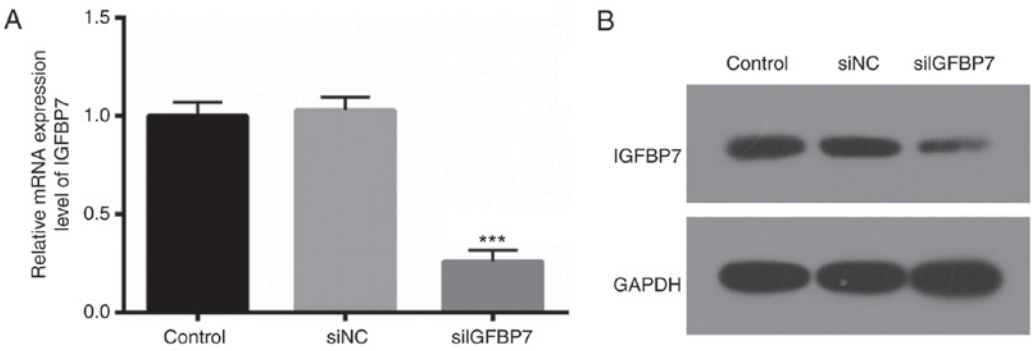

Figure 2. IGFBP7 was silenced in podocytes using small interfering RNA. (A) Relative mRNA expression level and (B) protein expression level of IGFBP7 in podocytes transfected with siNC and siIGFBP7. ***P<0.001 vs. siNC. IGFBP7, insulin-like growth factor-binding protein 7; siNC, normal control small interfering RNA; siIGFBP7, IGFBP7 small interfering RNA.

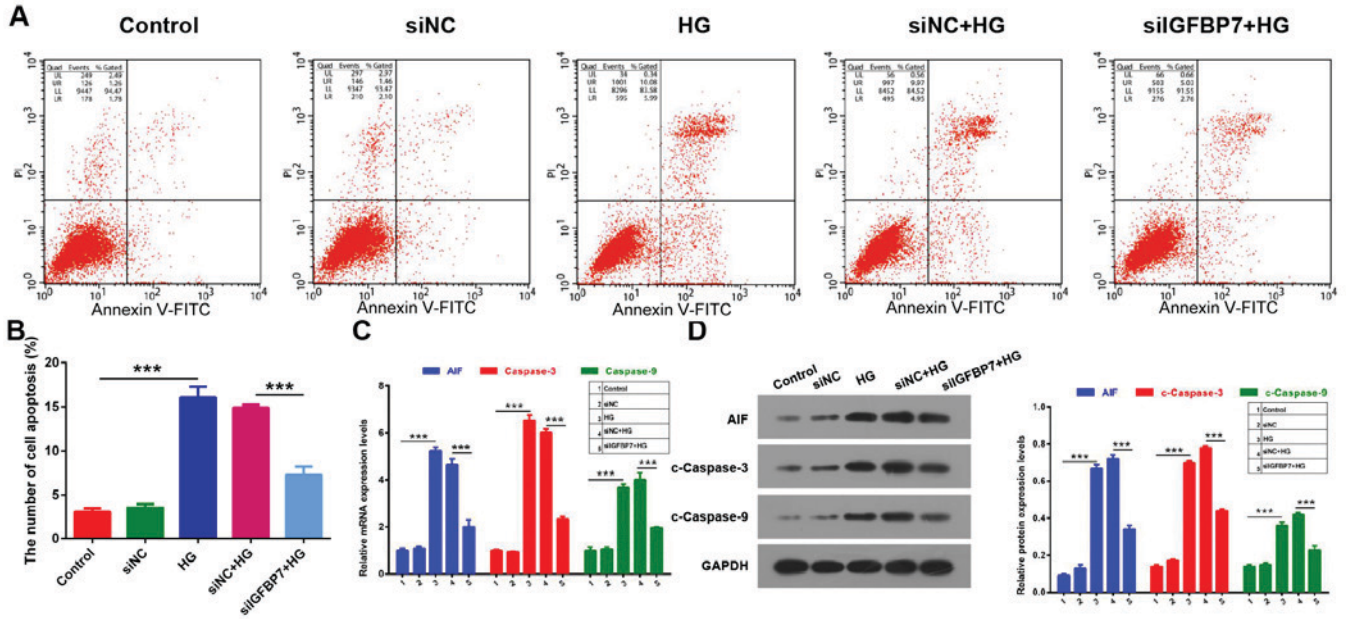

Figure 3. Silencing IGFBP7 inhibited apoptosis of podocytes mediated by HG. Podocytes were treated with PBS (control), siNC, 60 mM glucose (HG), siNC and HG, and siIGFBP7 and HG for 12 h. (A) Total apoptotic cells were measured using flow cytometry in treated podocytes. (B) Quantitative analysis of number of apoptotic cells. (C) AIF, caspase-3 and caspase-9 expression was detected via reverse transcription-quantitative polymerase chain reaction. (D) Western blotting of AIF, c-caspase-3 and c-caspase-9. Protein levels were quantified using densitometry. ***P<0.001. IGFBP7, insulin-like growth factor-binding protein 7; HG, high glucose; siNC, normal control small interfering RNA; siIGFBP7, IGFBP7 small interfering RNA; AIF, apoptosis inducing factor; c, cleaved; PI, propidium iodide; FITC, fluorescein isothiocyanate.

RT-qPCR and western blotting were then used to verify the IGFBP7 knockdown efficiency, and it was. demonstrated that IGFBP7 mRNA (Fig. 2A) and protein (Fig. 2B) expression was significantly (P<0.001) and markedly downregulated, respectively, in podocytes transfected with siIGFBP7, compared with siNC. These results indicated that the efficiency and specificity of siIGFBP7 was high.

IGFBP7 silencing inhibits apoptosis of podocytes mediated by HG. It wasthen detected whether IGFBP7 serves a role in the apoptosis of podocytes mediated by HG via apoptosis assay. The results demonstrated that the apoptotic ability was significantly increased in the HG group compared with control (P<0.001), and that IGFBP7 silencing significantly inhibited the apoptotic ability of podocytes induced by HG (P<0.001; Fig. 3A and B). In addition, the expression levels of three apoptosis-related genes (AIF, caspase-3 and caspase-9) were detected using RT-qPCR and western blotting. It was demonstrated that AIF, c-caspase-3 and c-caspase-9 expressions were significantly increased in the HG group compared with the control group, and that silencing IGFBP7 significantly downregulated expression of the three genes in podocytes induced by HG (P<0.001; Fig. 3C and D). These data indicated that silencing IGFBP7suppresses cell apoptosis of podocytes mediated by HG.

Silencing IGFBP7 inhibits EMT of podocytes induced by HG. To further investigate whether IGFBP7 participates in the process of cell EMT of podocytes, RT-qPCR and western blotting were used to analyze nephrin, p-cadherin, FSP-1, α-SMA and Snail expression. It was demonstrated that HG inhibited the expression of epithelial markers (nephrin and

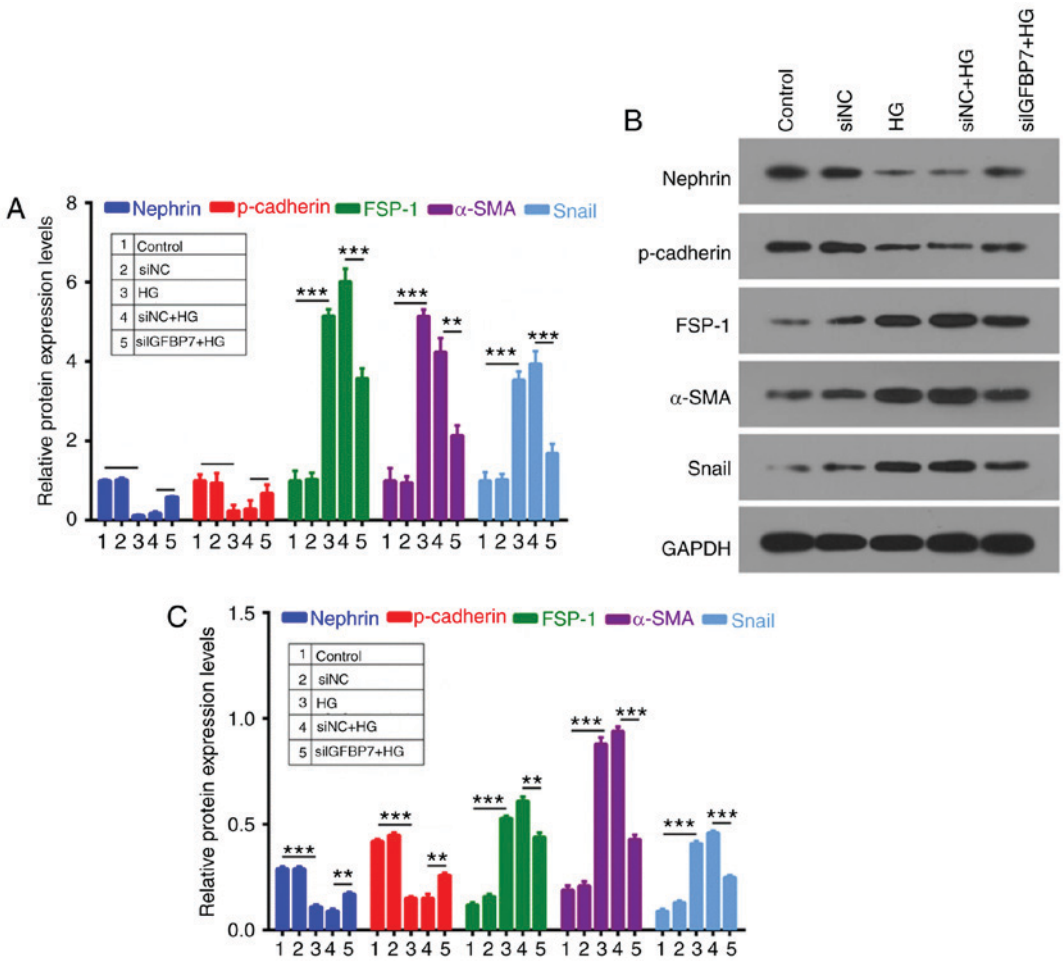

Figure 4. Silencing IGFBP7 inhibited epithelial mesenchymal transformation of podocytes induced by HG. Podocytes were treated with PBS (control), siNC, 60 mM glucose (HG), siNC and HG, and siIGFBP7 and HG for 12 h. (A) Reverse transcription-quantitative polymerase chain reaction was used to detect nephrin, p-cadherin, FSP-1, α-SMA and Snail expression in treated podocytes. Nephrin, p-cadherin, FSP-1, α-SMA, and Snail expressions were analyzed via (B) western blotting and (C) quantified. **P<0.01; ***P<0.001. IGFBP7, insulin-like growth factor-binding protein 7; HG, high glucose; siNC, normal control small interfering RNA; siIGFBP7, IGFBP7 small interfering RNA; p, phosphorylated; FSP-1, fibroblast-specific protein-1; α-SMA, α-smooth muscle actin.

p-cadherin) and promoted the expression of mesenchymal markers (FSP-1, α-SMA and Snail), which were reversed by silencing IGFBP7 (Fig. 4).

IGFBP7 silencing suppresses the TGF-β1/Smad pathway in podocytes induced by HG. TGF-β1/Smad signaling is associated with antimitotic activities in epithelial tissues (29). An ELISA assay was used to detect TGF-β1 concentration, which indicated that HG significantly increased TGF-β1 concentration, compared with controls (P<0.001), and IGFBP7 silencing significantly decreased TGF-β1 concentration (P<0.05; Fig. 5A). RT-qPCR and western blotting were then performed to measure the expression levels of TGF-β1 and Smad7, which indicated that HG significantly upregulated TGF-β1 expression, and significantly downregulated Smad7 expression, and that IGFBP7 silencing significantly reversed this HG-mediated regulation (P<0.001; Fig. 5B and C). In addition, protein expression levels of p-Smad3 and Smad3 were detected, and it was demonstrated that HG significantly promoted the phosphorylation of Smad3, and that IGFBP7 silencing further inhibited the phosphorylation of Smad3 induced by HG (P<0.001; Fig. 5D).

Discussion

DN is one of the main microvascular complications of diabetes mellitus, and it has been identified as a leading cause of end stage renal disease in the United States (30,31). Meanwhile, DN also is a serious threat to people's health in China (32,33). The elucidation of the pathogenesis of DN and the development of novel therapeutic measures are of importance for patients diagnosed with DN. The pathogenesis of DN is complex, and is associated with many factors, including hyperglycemia, lipid metabolism disorders, abnormal hemodynamics, inflammatory cytokines, oxidative stress and cell apoptosis (34-36). Following the construction of podocyte cell strains and the rising development of biochemical technology, podocytes have been increasingly used in research (37,38). Podocyte injury has been identified to serve an important role in the pathogenesis of DN and is considered as a pivotal factor for inducing proteinuria and glomerular sclerosis (5). This provides a novel approach for preventing and treating DN.

Podocytes are also known as glomerular visceral epithelial cells, which comprise the glomerular filtration barrier with a fenestrated endothelial layer and the glomerular basement

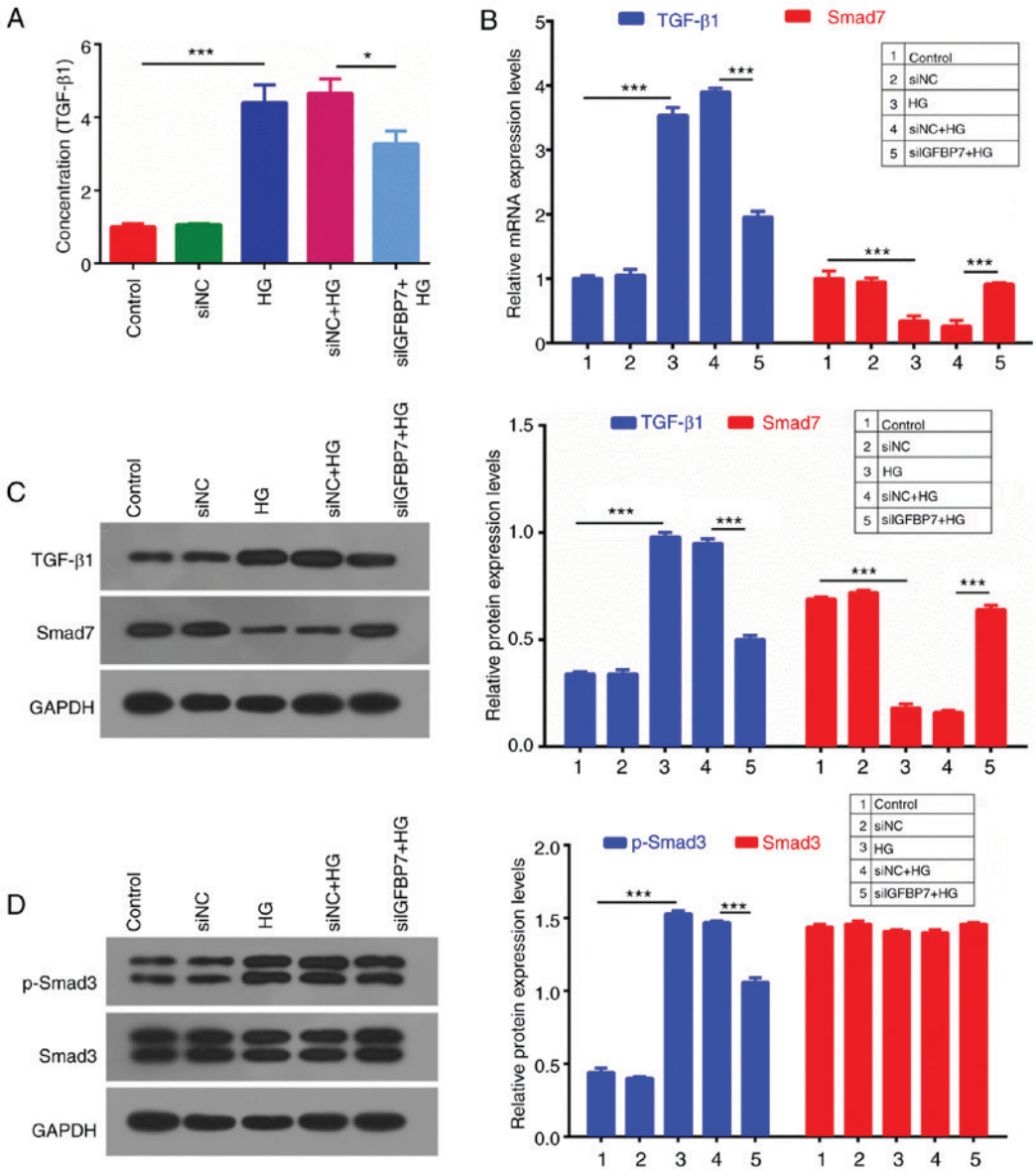

Figure 5. Silencing IGFBP7 suppressed the TGF-β1/Smad pathway in podocytes induced by HG. Podocytes were treated with PBS (control), siNC, 60 mM glucose (HG), siNC and HG, and siIGFBP7 and HG for 12 h. (A) TGF-β1 concentration was detected using ELISA. (B) The mRNA expression levels of TGF-β1 and Smad7 were analyzed using reverse transcription-quantitative polymerase chain reaction. (C) The protein expression levels of TGF-β1 and Smad7 were analyzed via western blotting. (D) The protein expression levels of p-Smad3 and Smad3 were analyzed via western blotting. *P<0.05; ***P<0.001. IGFBP7, insulin-like growth factor-binding protein 7; TGF-Smad7 were analyzed via western bloSmad, mothers against decapentaplegic homolog; HG, high glucose; siNC, normal control small interfering RNA; siIGFBP7, IGFBP7 small interfering RNA; p, phosphorylated.

membrane (5). Podocytes are highly differentiated cells and have a limited proliferative ability (39). When the number of exfoliative cells exceeds that of proliferative cells, the glomerular filtration barrier is destroyed, which leads to massive proteinuria, excretion of collagen IV by podocytes, and ultimately glomerular sclerosis (40). Hyperglycemia, angiotensin II, lipid metabolism disorder, oxidative stress and inflammatory cytokines stimulate podocytes to be dysfunctional and impaired (41). Podocytes also have a variety of specific markers, such as synaptopodin, Wilms tumor protein, glomerular epithelial protein-1, nephrin, podocalyxin, and C3b (42). Among them, synaptopodin is a protein coupling with actin microfilament, which is located in glomerular podocytes and hindbrain synapses (43,44). The present study demonstrated that synaptopodin was highly expressed in podocytes, and that HG promoted podocyte proliferation in a time-dependent and dose-dependent manner.

IGFBP7 has binding affinities to IGFs and has been demonstrated to either positively or negatively regulate the IGF signaling pathway, and serve a crucial role in cell growth, differentiation and development in an IGF-independent manner (45). It has also been demonstrated that IGFBP7 serves an important role in DN, for example, IGFBP7 is associated with the process of human renal proximal tubular epithelial cells via Smad2/4 (46). However, the role of IGFBP7 in DN is yet to be elucidated. In the present study, IGFBP7 expression in podocytes was blocked via transfection with siRNA, which reduced the HG-induced increase of podocyte apoptosis. HG also increased AIF, c-caspase-3 and c-caspase-9 expression, which was ameliorated by IGFBP7 silencing.

A number of previous studies have suggested that EMT serves a role podocyte depletion in DN, which is responsible for the onset of proteinuria (47-49). It has been demonstrated that TGF-β significantly promotes EMT by reducing levels of epithelial markers (nephrin and p-cadherin) and increasing mesenchymal marker (FSP-1) levels (50,51). Furthermore, α-SMA is also a mesenchymal marker (52). Snail is a pivotal transcriptional factor that participates in initiating EMT (11,16,17,53,54). In the present study, it was demonstrated that HG significantly inhibited nephrin and p-cadherin expressions, and promoted the expressions of FSP-1, α-SMA and Snail, which was ameliorated by IGFBP7 silencing. This suggested that silencing IGFBP7 inhibited EMT of podocytes induced by HG.

The cytokines of the TGF-β family have a number of biological effects through different signal transduction pathways, among which, the Smad protein family serves an important role (55). The process of transmembrane signaling depends on the Smad protein family, which regulates expression of a number of genes (56). In the present study, the expression of TGF-β1 and its signal transduction elements (Smad2/3 and Smad7) was examined, and renal extracellular matrix accumulation in the renal tissues of experimental diabetes was assessed to further clarify the effects of Smads on the development of DN. It was demonstrated that HG significantly upregulated TGF-β1 expression, promoted phosphorylation of Smad3 and downregulated Smad7 expression, which was ameliorated by IGFBP7 silencing.

In conclusion, the present study indicated that glucose facilitated podocyte proliferation in a time-dependent and dose-dependent manner, and that IGFBP7 silencing inhibited apoptosis and EMT of podocytes mediated by HG via suppressing the TGF-β1/Smad pathway. However, it is not yet clear how GFBP7 regulates caspases and EMT-related factors, and the specific molecular mechanism of IGFBP7 in the apoptosis and EMT of podocytes should be explored in further studies. The present study provides further elucidation and a theoretical basis for novel diagnostic and treatment options for DN.

Acknowledgements

Not applicable.

Funding

No funding was received.

Availability of data and materials

The datasets used and/or analyzed during the current study are available from the corresponding author on reasonable request.

Authors' contributions

XJC, LW and XLW were responsible for the design of the experimental scheme. XLW and FYH were responsible for analyzing and interpreting data . XJC was involved in drafting the manuscript. All authors were responsible for giving final approval of the version to be published

Ethics approval and consent to participate

Not applicable.

Patient consent for publication

Not applicable.

Competing interests

The authors declare that they have no competing interests.

References

1. Zheng S, Powell DW, Zheng F, Kantharidis P and Gnudi L: Diabetic nephropathy: Proteinuria, inflammation, and fibrosis. J diabetes Res 2016: 5241549, 2016.
2. Wang S, Li Y, Zhao J, Zhang J and Huang Y: Mesenchymal stem cells ameliorate podocyte injury and proteinuria in a type 1 diabetic nephropathy rat model. Biol Blood Marrow Transplant 19: 538-546, 2013.
3. Yasuda-Yamahara M, Kume S, Tagawa A, Maegawa H and Uzu T: Emerging role of podocyte autophagy in the progression of diabetic nephropathy. Autophagy 11: 2385-2386, 2015.
4. Zhao L, Wang X, Sun L, Nie H, Liu X, Chen Z and Guan G: Critical role of serum response factor in podocyte epithelial-mesenchymal transition of diabetic nephropathy. Diab Vasc Dis Res 13: 81-92, 2016.
5. Yasuno K, Kamiie J and Shirota K: Analysis of ultrastructural glomerular basement membrane lesions and podocytes associated with proteinuria and sclerosis in osborne-mendel rats with progressive glomerulonephropathy. J Vet Sci 14: 223-226, 2013.
6. Huang L, You YS and Wu W: Role of CD2-associated protein in podocyte apoptosis and proteinuria induced by angiotensin II. Ren Fail 36: 1328-1332, 2014.
7. Tagawa A, Yasuda M, Kume S, Yamahara K, Nakazawa J, Chin-Kanasaki M, Araki H, Araki S, Koya D, Asanuma K, *et al*: Impaired podocyte autophagy exacerbates proteinuria in diabetic nephropathy. Diabetes 65: 755-767, 2016.
8. Liao R, Liu Q, Zheng Z, Fan J, Peng W, Kong Q, He H, Yang S, Chen W, Tang X and Yu X: Tacrolimus protects podocytes from injury in lupus nephritis partly by stabilizing the cytoskeleton and inhibiting podocyte apoptosis. PloS One 10: e0132724, 2015.
9. Chitra PS, Swathi T, Sahay R, Reddy GB, Menon RK and Kumar PA: Growth hormone induces transforming growth factor-beta-induced protein in podocytes: Implications for podocyte depletion and proteinuria. J Cell Biochem 116: 1947-1956, 2015.
10. Ziyadeh FN and Wolf G: Pathogenesis of the podocytopathy and proteinuria in diabetic glomerulopathy. Curr Diabetes Rev 4: 39-45, 2008.
11. Yamaguchi Y, Iwano M, Suzuki D, Nakatani K, Kimura K, Harada K, Kubo A, Akai Y, Toyoda M, Kanauchi M, *et al*: Epithelial-mesenchymal transition as a potential explanation for podocyte depletion in diabetic nephropathy. Am J Kidney Dis 54: 653-664, 2009.
12. Faul C, Asanuma K, Yanagida-Asanuma E, Kim K and Mundel P: Actin up: Regulation of podocyte structure and function by components of the actin cytoskeleton. Trends Cell Biol 17: 428-437, 2007.
13. Li Y, Kang YS, Dai C, Kiss LP, Wen X and Liu Y: Epithelial-to-mesenchymal transition is a potential pathway leading to podocyte dysfunction and proteinuria. Am J Pathol 172: 299-308, 2008.
14. Pavenstadt H, Kriz W and Kretzler M: Cell biology of the glomerular podocyte. Physiol Rev 83: 253-307, 2003.
15. Durvasula RV and Shankland SJ: Podocyte injury and targeting therapy: An update. Curr Opin Nephrol Hypertens 15: 1-7, 2006.
16. Kang YS, Li Y, Dai C, Kiss LP, Wu C and Liu Y: Inhibition of integrin-linked kinase blocks podocyte epithelial-mesenchymal transition and ameliorates proteinuria. Kidney Int 78: 363-373, 2010.
17. Susztak K, Raff AC, Schiffer M and Bottinger EP: Glucose-induced reactive oxygen species cause apoptosis of podocytes and podocyte depletion at the onset of diabetic nephropathy. Diabetes 55: 225-233, 2006.

18. Chen LH, Liu DW, Chang JL, Chen PR, Hsu LP, Lin HY, Chou YF, Lee CF, Yang MC, Wen YH, *et al*: Methylation status of insulin-like growth factor-binding protein 7 concurs with the malignance of oral tongue cancer. J Exp Clin Cancer Res 34: 20, 2015.
19. Honore PM, Nguyen HB, Gong M, Chawla LS, Bagshaw SM, Artigas A, Shi J, Joannes-Boyau O, Vincent JL, Kellum JA and Sapphire and: Topaz Investigators: Urinary tissue inhibitor of metalloproteinase-2 and insulin-like growth factor-binding protein 7 for risk stratification of acute kidney injury in patients with sepsis. Crit Care Med 44: 1851-1860, 2016.
20. Jiang J, Chen Z, Liang B, Yan J, Zhang Y, Xu H, Huang Y and Jiang H: The change of circulating insulin like growth factor binding protein 7 levels may correlate with postoperative cognitive dysfunction. Neurosci Lett 588: 125-130, 2015.
21. Li N, Zhang Z, Zhang L, Wang S, Zou Z, Wang G and Wang Y: Insulin-like growth factor binding protein 7, a member of insulin-like growth factor signal pathway, involved in immune response of small abalone haliotis diversicolor. Fish Shellfish Immunol 33: 229-242, 2012.
22. Tamura K, Yoshie M, Hashimoto K and Tachikawa E: Inhibitory effect of insulin-like growth factor-binding protein-7 (IGFBP7) on in vitro angiogenesis of vascular endothelial cells in the rat corpus luteum. J Reprod Dev 60: 447-453, 2014.
23. Yuan L, Fan WJ, Yang XG, Rao SM, Song JL and Song GH: Inhibitory effect of exogenous insulin-like growth factor binding protein 7 on proliferation of human breast cancer cell line MDA-MB-453 and its mechanism. Sheng Li Xue Bao 65: 519-524, 2013 (In Chinese).
24. Bolomsky A, Hose D, Schreder M, Seckinger A, Lipp S, Klein B, Heintel D, Ludwig H and Zojer N: Insulin like growth factor binding protein 7 (IGFBP7) expression is linked to poor prognosis but may protect from bone disease in multiple myeloma. J Hematol Oncol 8: 10, 2015.
25. Tian X, Zhang L, Sun L, Xue Y and Xie S: Low expression of insulin-like growth factor binding protein 7 associated with poor prognosis in human glioma. J Int Med Res 42: 651-658, 2014.
26. Chen D, Siddiq A, Emdad L, Rajasekaran D, Gredler R, Shen XN, Santhekadur PK, Srivastava J, Robertson CL, Dmitriev I, *et al*: Insulin-like growth factor-binding protein-7 (IGFBP7): A promising gene therapeutic for hepatocellular carcinoma (HCC). Mol Ther 21: 758-766, 2013.
27. Georges RB, Adwan H, Hamdi H, Hielscher T, Linnemann U and Berger MR: The insulin-like growth factor binding proteins 3 and 7 are associated with colorectal cancer and liver metastasis. Cancer Biol Ther 12: 69-79, 2011.
28. Livak KJ and Schmittgen TD: Analysis of relative gene expression data using real-time quantitative PCR and the 2(-Delta Delta C(T)) method. Methods 25: 402-408, 2001.
29. Yu Z, Tang Y, Hu D and Li J: Inhibitory effect of genistein on mouse colon cancer MC-26 cells involved TGF-beta1/Smad pathway. Biochem Biophys Res Commun 333: 827-832, 2005.
30. Satirapoj B and Adler SG: Prevalence and management of diabetic nephropathy in western countries. Kidney Dis (Basel) 1: 61-70, 2015.
31. Tomino Y and Gohda T: The Prevalence and management of diabetic nephropathy in asia. Kidney Dis (Basel) 1: 52-60, 2015.
32. Chen L, Su W, Chen H, Chen DQ, Wang M, Guo Y and Zhao YY: Proteomics for biomarker identification and clinical application in kidney disease. Adv Clin Chem 85: 91-113, 2018.
33. Han Q, Zhang J, Wang Y, Li H, Zhang R, Guo R, Li L, Teng G, Wang J, Wang T and Liu F: Thyroid hormones and diabetic nephropathy: An essential relationship to recognize. Nephrology (Carlton) 2018.
34. Varga ZV, Giricz Z, Liaudet L, Hasko G, Ferdinandy P and Pacher P: Interplay of oxidative, nitrosative/nitrative stress, inflammation, cell death and autophagy in diabetic cardiomyopathy. Biochim Biophys Acta 1852: 232-242, 2015.
35. Flyvbjerg A: The role of the complement system in diabetic nephropathy. Nat Rev Nephrol 13: 311-318, 2017.
36. Wada J and Makino H: Inflammation and the pathogenesis of diabetic nephropathy. Clin Sci (Lond) 124: 139-152, 2013.
37. Imasawa T, Obre E, Bellance N, Lavie J, Imasawa T, Rigothier C, Delmas Y, Combe C, Lacombe D, Benard G, *et al*: High glucose repatterns human podocyte energy metabolism during differentiation and diabetic nephropathy. FASEB J 31: 294-307, 2017.
38. Li JJ, Kwak SJ, Jung DS, Kim JJ, Yoo TH, Ryu DR, Han SH, Choi HY, Lee JE, Moon SJ, *et al*: Podocyte biology in diabetic nephropathy. Kidney Int (Suppl) S36-S42, 2007.
39. Zhang Y, Chen Y, Yang F and Zhou J: HBx transfection limits proliferative capacity of podocytes through cell cycle regulation. Acta Biochim Biophys Sin (Shanghai) 46: 1016-1023, 2014.
40. Anders HJ, Vielhauer V and Schlondorff D: Chemokines and chemokine receptors are involved in the resolution or progression of renal disease. Kidney Int 63: 401-415, 2003.
41. Ferder L, Inserra F and Martinez-Maldonado M: Inflammation and the metabolic syndrome: Role of angiotensin II and oxidative stress. Curr Hypertens Rep 8: 191-198, 2006.
42. Yang Y, Gubler MC and Beaufils H: Dysregulation of podocyte phenotype in idiopathic collapsing glomerulopathy and HIV-associated nephropathy. Nephron 91: 416-423, 2002.
43. Madne TH and Dockrell MEC: Human podocytes responses to alternatively spliced Extra domain A Fibronectin in culture. Cell Mol Biol (Noisy-le-Grand) 64: 45-52, 2018.
44. Rochman M, Travers J, Abonia JP, Caldwell JM and Rothenberg ME: Synaptopodin is upregulated by IL-13 in eosinophilic esophagitis and regulates esophageal epithelial cell motility and barrier integrity. JCI Insight 2: 96789, 2017.
45. Chen D, Yoo BK, Santhekadur PK, Gredler R, Bhutia SK, Das SK, Fuller C, Su ZZ, Fisher PB and Sarkar D: Insulin-like growth factor-binding protein-7 functions as a potential tumor suppressor in hepatocellular carcinoma. Clin Cancer Res 17: 6693-6701, 2011.
46. Watanabe J, Takiyama Y, Honjyo J, Makino Y, Fujita Y, Tateno M and Haneda M: Role of IGFBP7 in diabetic nephropathy: TGF-β1 induces IGFBP7 via smad2/4 in human renal proximal tubular epithelial cells. PloS One 11: e0150897, 2016.
47. Chang YP, Sun B, Han Z, Han F, Hu SL, Li XY, Xue M, Yang Y, Chen L, Li CJ and Chen LM: Saxagliptin attenuates albuminuria by inhibiting podocyte epithelial-to-mesenchymal transition via sdf-1α in diabetic nephropathy. Front Pharmacol 8: 780, 2017.
48. Chen T, Zheng LY, Xiao W, Gui D, Wang X and Wang N: Emodin ameliorates high glucose induced-podocyte epithelial-mesenchymal transition in-vitro and in-vivo. Cell Physiol Biochem 35: 1425-1436, 2015.
49. Du M, Wang Q, Li W, Ma X, Wu L, Guo F, Zhao S, Huang F, Wang H and Qin G: Overexpression of FOXO1 ameliorates the podocyte epithelial-mesenchymal transition induced by high glucose in vitro and in vivo. Biochem Biophys Res Commun 471: 416-422, 2016.
50. Chen Q, Yang W, Wang X, Li X, Qi S, Zhang Y and Gao MQ: TGF-β1 induces emt in bovine mammary epithelial cells through the TGFβ1/smad signaling pathway. Cell Physiol Biochem 43: 82-93, 2017.
51. Ibrini J, Fadel S, Chana RS, Brunskill N, Wagner B, Johnson TS and El Nahas AM: Albumin-induced epithelial mesenchymal transformation. Nephron Exp Nephrol 120: e91-102, 2012.
52. Igietseme JU, Omosun Y, Nagy T, Stuchlik O, Reed MS, He Q, Partin J, Joseph K, Ellerson D, George Z, *et al*: Molecular pathogenesis of chlamydia disease complications: Epithelial-mesenchymal transition and fibrosis. Infect Immun 86: e00585, 2017.
53. Wiggins RC: The spectrum of podocytopathies: A unifying view of glomerular diseases. Kidney Int 71: 1205-1214, 2007.
54. Yu D, Petermann A, Kunter U, Rong S, Shankland SJ and Floege J: Urinary podocyte loss is a more specific marker of ongoing glomerular damage than proteinuria. J Am Soc Nephrol 16: 1733-1741, 2005.
55. Kamato D, Burch ML, Piva TJ, Rezaei HB, Rostam MA, Xu S, Zheng W, Little PJ and Osman N: Transforming growth factor-beta signalling: role and consequences of Smad linker region phosphorylation. Cell Signal 25: 2017-2024, 2013.
56. Ning W, Tao L, Liu C, Sun J, Xiao Y, Hu J, Chen J, Zheng X and Wang W: Effect of enalapril on the expression of TGF-beta1, p-Smad2/3 and Smad7 in renal interstitial fibrosis in rats. Zhong Nan Da Xue Xue Bao Yi Xue Ban 34: 27-34, 2009 (In Chinese).